Chalmers University of Technology
Department of Materials and Manufacturing Technology

Examination in Phase Transformations MMK162
Advanced Engineering Materials
14.00-18.00, 25 October 2013

Aid permitted at examination: Electronic calculator of the simple type approved by Chalmers

Solutions and answers should be well worked out and <u>motivated</u> to get full credit.

The question pages must be submitted together with the written answers.
In the headlines below preliminary credits are given, this might be changed during correction.
Solutions will be displayed on course homepage.

Assignments	Credit
1. Phase diagrams and free energy curves	7
2. Diffusion	9
3. Interfaces and microstructure	8
4. Solidification	10
5. Diffusional transformations	7
6. Diffusionless transformation	3
7. Novel metallic materials	3
8. Solid/gas interactions	3
Sum:	**50**

Limits for: 3>45%
4>60%
5>75%

Grading will be based on the total sum of **60 points:** points for practical class (max 4p) and project essay (max 6p) will be added to the exam points (max 50p). Bonus points earned during lectures (quiz) will be added to the exam points.

Göteborg, 2013.10.22

Eduard Hryha

1. Phase diagrams and free energy curves (8 p)

a) Derive phase diagram for Cu-Ag system using free energy diagrams according to the figure below. Respective temperatures are 1400, 1358, 1235, 1100, 1052 and 900K (marked on the top of each figure). X and Y-axes should be drawn in correct scale compared to the phase diagram. (6)
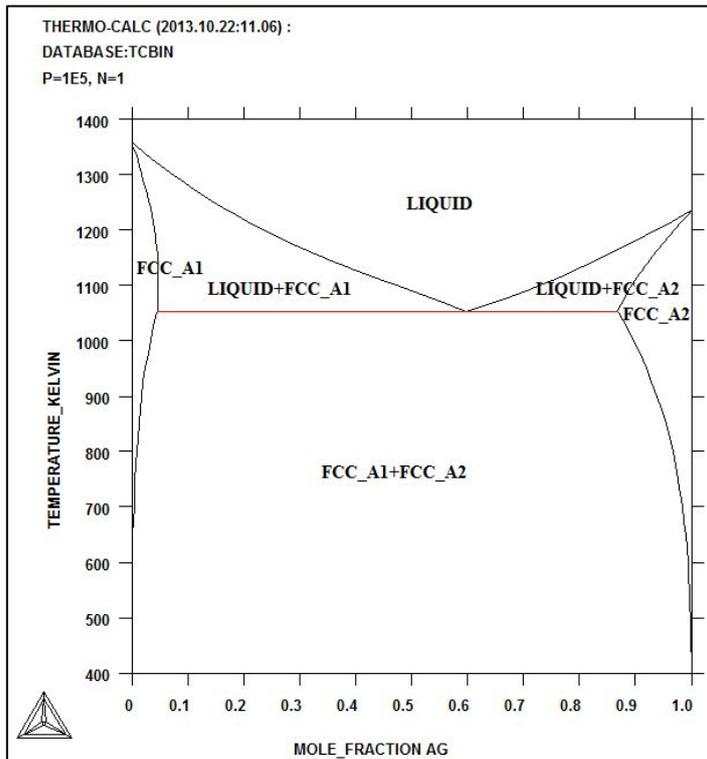
Draw tangents to the G-curves and mark points of intersection as shown below:
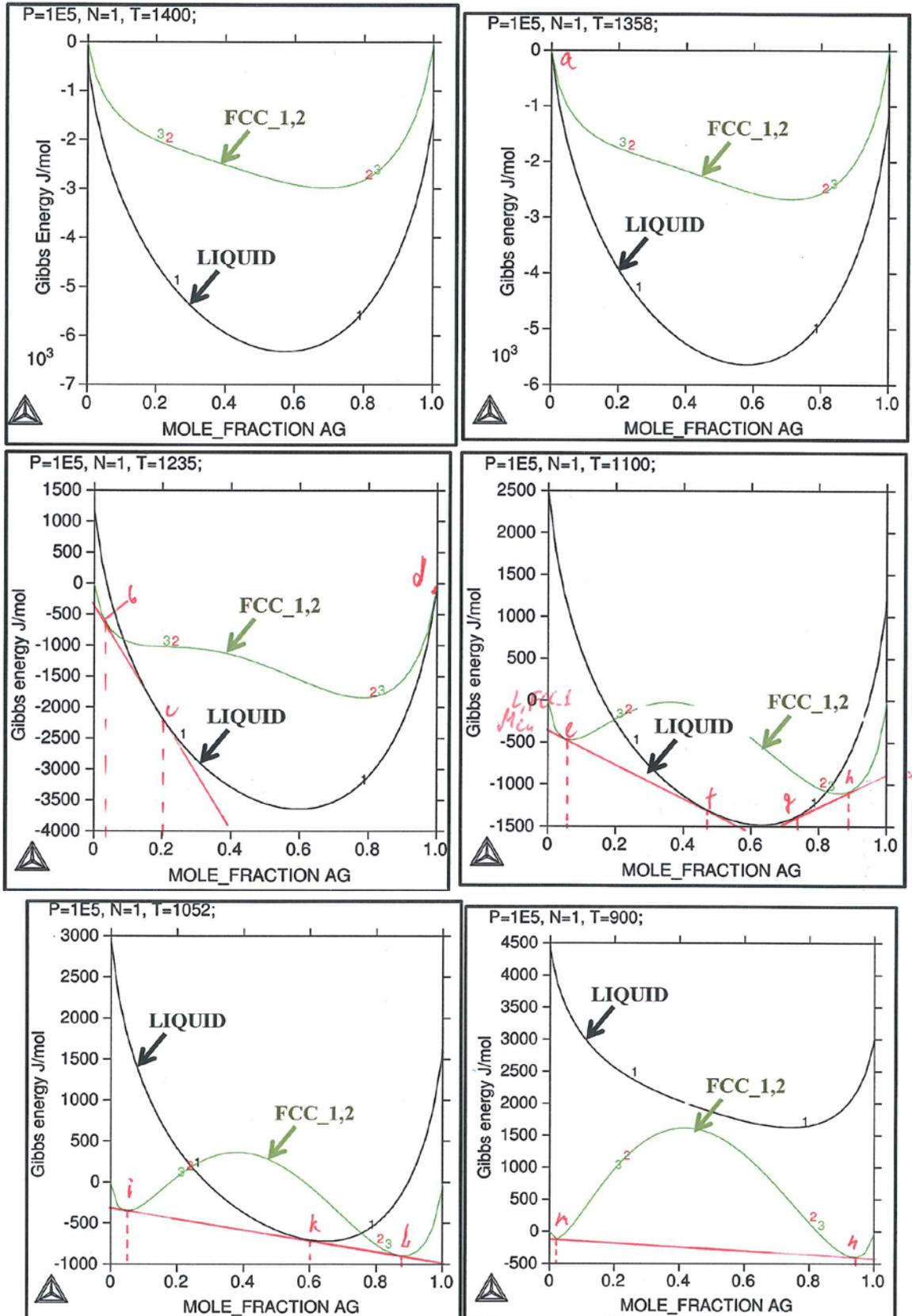
Draw diagram based on marked points on the G-graphs above as presented below:
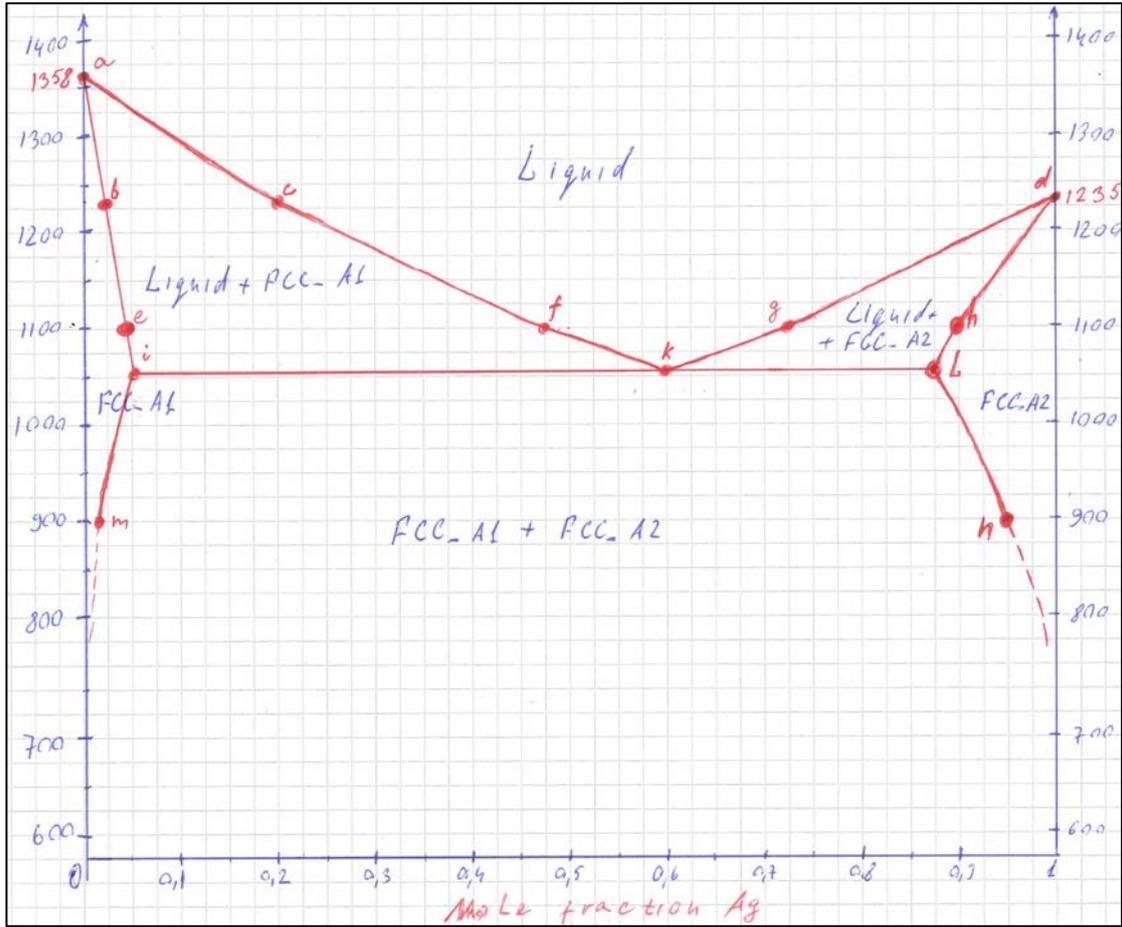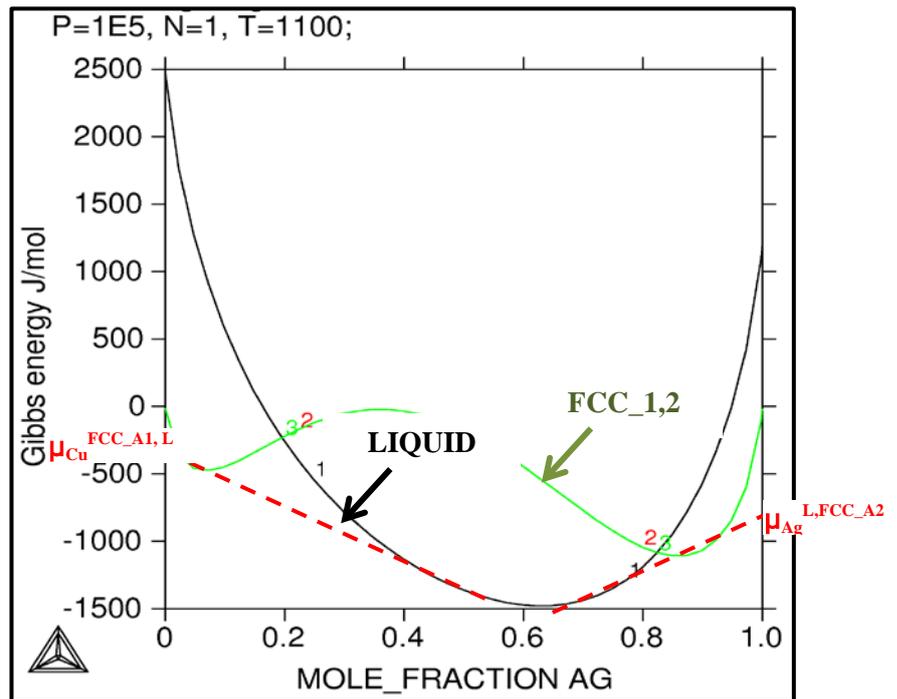

Phase diagram from ThermoClac:

b) Mark chemical potentials of the phase equilibriums for the free energy diagrams at 1100K. (1 p)

See figure:

c) How similar is crystallographic structure of the Cu-rich FCC_1 and Ag-rich FCC_2? How is that reflected on G-curve? Short motivation is necessary to get full credit. (1 p)

Cu-rich FCC_A1 and Ag-rich FCC_A2 have the same FCC structure with only difference in lattice parameter (hence, marked as FCC_A1 and FCC_A2) – this result in the common G-curve for both. In case elements A and B have different crystallographic structures – each structure will have its own G-curves and so two separate G-curves will be present on the graphs above.

2. Diffusion (9 p)

a) Sketch Gibbs free energy diagram and based on it describe "uphill" diffusion – driving force, direction of the atom movement and way to determine it, effect on concentration, etc. Motivation is necessary to get full credit. (3 p)
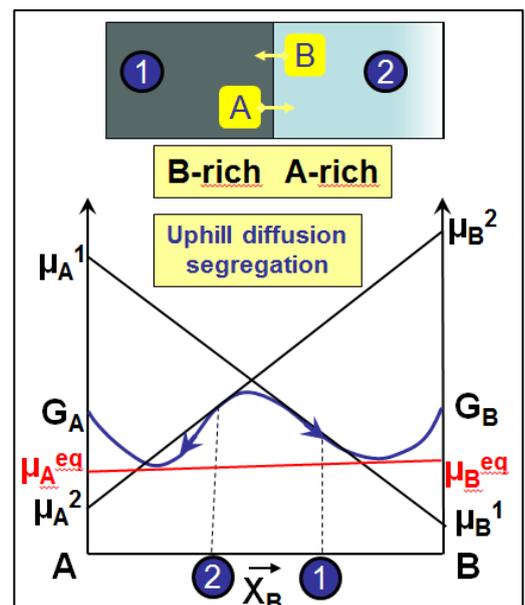
"Uphill" diffusion is typical for alloys containing miscibility gap.

Gibbs free energy diagram – see Fig:

Driving force: constant chemical potential, μ, or lowest G in the whole volume.
- diffusion from the **low** concentration **to high** concentration;
- this leads to **increased** compositional differences.

Diffusion always down towards chemical potential!!!

4

b) Calculate and sketch concentration profile of carbon after decarburization of steel at 900°C for 30 min. Carbon potential of the processing atmosphere is constant and equal to 0.1%. Carbon content of the steel is 1%. Diffusion coefficient of carbon in austenite is $D=2.39*10^{-11}$ m^{2}s^{-1}. Calculate values of the carbon content for as minimum 5 depths and based on it sketch approximate graph of carbon profile. (6p).

**Table 5.3** Table of the error function

z	erf z	z	erf z	z	erf z	z	erf z
0	0	0.40	0.4284	0.85	0.7707	1.6	0.9763
0.025	0.0282	0.45	0.4755	0.90	0.7970	1.7	0.9838
0.05	0.0564	0.50	0.5205	0.95	0.8209	1.8	0.9891
0.10	0.1125	0.55	0.5633	1.0	0.8427	1.9	0.9928
0.15	0.1680	0.60	0.6039	1.1	0.8802	2.0	0.9953
0.20	0.2227	0.65	0.6420	1.2	0.9103	2.2	0.9981
0.25	0.2763	0.70	0.6778	1.3	0.9340	2.4	0.9993
0.30	0.3286	0.75	0.7112	1.4	0.9523	2.6	0.9998
0.35	0.3794	0.80	0.7421	1.5	0.9661	2.8	0.9999

Carbon profile in case of decarburization: $C = C_0 erf \dfrac{x}{2\sqrt{Dt}}$ is valid only in case when carbon potential of the processing gas is equal to C$_S$=0!!!

However, in case you have defined carbon potential of the atmosphere (0.1 %C) – you have to use the same equation as for carburization $C = C_s - (C_s - C_0) erf \dfrac{x}{2\sqrt{Dt}}$ where C$_s$=0.1%C and C$_0$=1%C. To simplify calculations it is easier to choose values of *z* and respective values of *erf(z)* from table of values of error function. Then, by knowing the value of z and Dt you can calculate depth x. By knowing the value of *erf(z)* you can calculate C. The sketch of carbon profile is presented below the table.

C$_0$	Cs	z	erf	D	t, s	Dt	2sqrt(Dt)	C	x (mm)
1	0.1	0	0	2.39E-11	1800	4.3E-08	0.000415	0.1	0
1	0.1	0.05	0.0564	2.39E-11	1800	4.3E-08	0.000415	0.15076	0.020741
1	0.1	0.1	0.1125	2.39E-11	1800	4.3E-08	0.000415	0.20125	0.041483
1	0.1	0.5	0.5205	2.39E-11	1800	4.3E-08	0.000415	0.56845	0.207413
1	0.1	0.75	0.7112	2.39E-11	1800	4.3E-08	0.000415	0.74008	0.311119
1	0.1	1	0.8427	2.39E-11	1800	4.3E-08	0.000415	0.85843	0.414825
1	0.1	2	0.9953	2.39E-11	1800	4.3E-08	0.000415	0.99577	0.829651
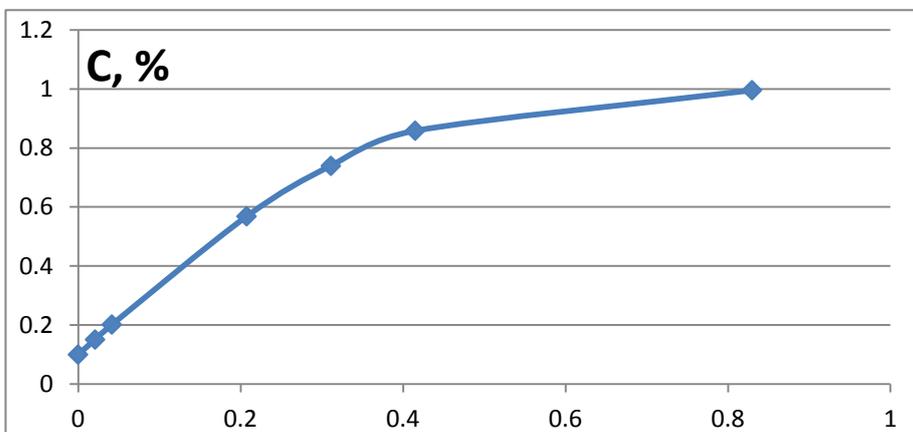
3. Interfaces and microstructure (8p)

a) Describe the main differences between the low-, high- and special-angle grain boundaries, their surface energy and mobility. (3 p).

- Low angle grain boundary - misorientation between two grains small → array of dislocations. Energy of boundary is equal to the total energy of dislocations within unit area of boundary.

- Energy of boundary depends on the spacing of dislocations D → $D = \dfrac{b}{\sin\theta} \approx \dfrac{b}{\theta}$

- At very small θ, γ is proportional to the dislocation density in the boundary: $\gamma_b \propto \dfrac{1}{D} \propto \theta$

- As θ increases → strain field of disslocations progressively cancel → γ increases at decreasing rate;

- at θ>10-15° - dislocatioon cores overlap → impossible to identify individual dislocations → γ_b is almost independant on θ.

- At θ>10-15° → **_random high angle boundary_** → poor fit, relatively open structure, bonds between atoms are brocken or highly distorted → high γ_b, γ_b is almost independent of θ:

- Measured high-angle GB energies, γ_b, ar often found to be $\gamma_b \approx 1/3\ \gamma_{sv}$;
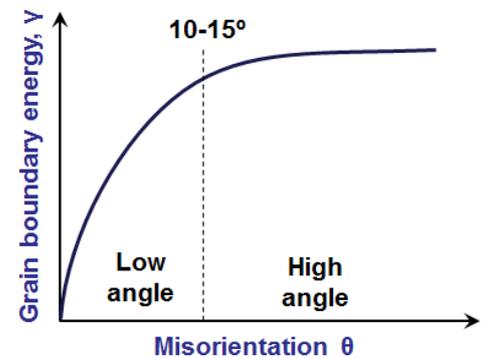
Special High-Angle Grain Boundaries → have lower energy than random high-angle grain boundaries → particular missorientations allowing good fit between adjoining lattices. Example is coherent twin boundary, for example in fcc at θ= 70.5° around <110>. Energy of twin boundary is very sensitive to orientation → if twin boundary does not lie exactly paralel to the twinning plane – incoherent twin boundary:
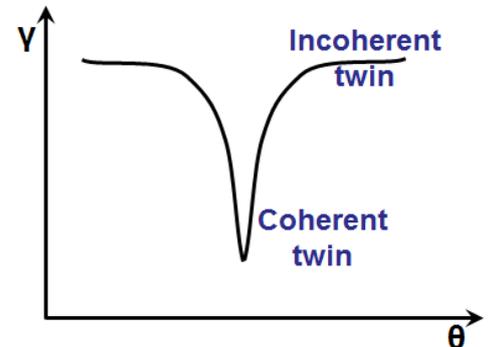
-
- Random high angle boundary – open structure and so high mobility than low-angle or special high-angle grain boundaries;
- Special high angle boundary – low mobility but _can_ have higher mobility than random if impurities stick to random high angle boundaries!

b) Explain kinetics of the grain growth, namely: driving force, normal and abnormal grain growth, effect of secondary particles on the grain growth and factors influencing stabilization of the fine-grained structure. Presentation of the relevant equations, schematics representation of the effect of secondary particles as well as motivation of the answer are necessary to get full credit. (5 p).

At sufficiently high temperature (T>0.5 T_m) GB will migrate in order to reduce G. Rate at which mean grain diameter $\bar{D}$ increase depends on GB mobility and driving force for migration.

Assuming that mean radius of curvature r is proportional to $\bar{D}$ → mean driving force is proportional to $2\gamma/\bar{D}$: $\dfrac{\Delta G}{V_m} = F = \dfrac{2\gamma}{r}$ and hence velocity of GB migration: $v = \alpha M \dfrac{2\gamma}{\bar{D}} \cong \dfrac{d\bar{D}}{dt}$

Integration taking $\bar{D} = D_0$ when t=0 gives: $\bar{D}^2 = \bar{D}_0^2 + 4\alpha M\gamma \cdot t$. Experimentally found that grain growth in pure metals follows: $\bar{D} = K't^n$ where n ≈ 0.5 only for very pure metals or at very high temperatures, otherwise n << 0.5.

Description of the thermally activated grain growth, presented above, is valid for **normal** grain growth. A**bnormal** grain growth → growth of just a few grains to very large diameters (discontinuous grain growth, coarsening or secondary recrystallization) – happens when normal grain growth ceases due to the presence of fine particulate array.

In case of presence of secondary particles on grain boundaries, GB is attached to the particle along a length $2\pi r \cos\theta$ and so particle exert pulling force $P = \pi r\gamma$ when $\sin\theta \cos\theta \to max$ ($\theta = 45°$).
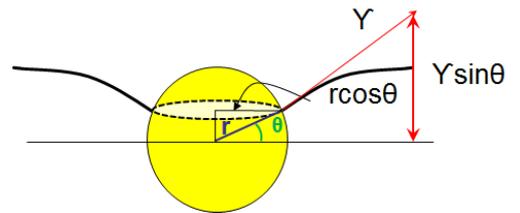
Restraining force on boundary by particle drag oppose driving force for the grain growth ($\sim 2\gamma/\bar{D}$) is $\dfrac{2\gamma}{\bar{D}} = \dfrac{3f\gamma}{2r}$ (where f is the volume fraction of particles with radius r). Hence, maximum grain size can be evaluated as $\bar{D}_{max} = \dfrac{4r}{3f}$.

Stabilization of fine grain size requires large volume fraction of very small particles: $\bar{D}_{max} = \dfrac{4r}{3f}$. If temperature is too high particles tend to coarsen or dissolve and as a result abnormal grain growth can occur.
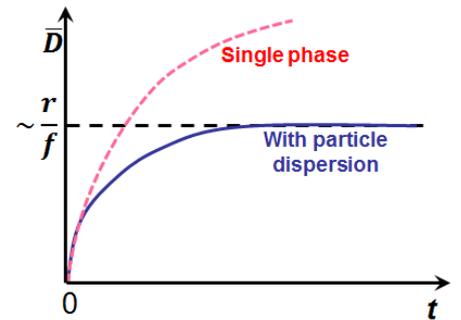

4. Solidification (10p)

a) Describe heterogeneous nucleation in solids – use the case of heterogeneous nucleation on a flat mould.

    i. Sketch the balance between interfacial tensions and describe schematically how tensions are balanced. (2 p)

Total interfacial energy is minimized if embryo has a shape of spherical cap with a "wetting" angle θ → interfacial tensions must be balanced:

$\cos\theta = \dfrac{\gamma_{ML} - \gamma_{SM}}{\gamma_{SL}}$
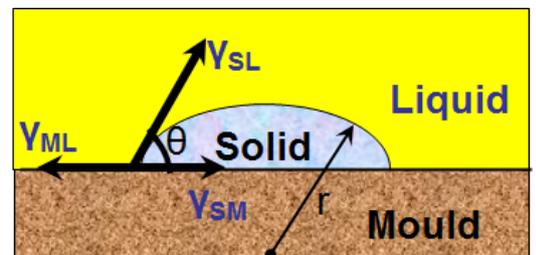
    ii. Describe change in the free energy connected to the formation of such embryo and effect of different terms on total excess free energy. (2p)

Formation of embryo is associated with the excess free energy:

$$\Delta G_{Het} = -V_S \Delta G_v + A_{SL}\gamma_{SL} + A_{SM}\gamma_{SM} - A_{SM}\gamma_{ML}$$

The same written in terms of the wetting angle $\boldsymbol{\theta}$ and cap radius r:

$$\Delta G_{Het} = \left\{ -\frac{4}{3}\pi r^3 \Delta G_v + 4\pi r^2 \gamma_{SL} \right\} S(\theta)$$

Shape factor (depends only on $\boldsymbol{\theta}$): $\boldsymbol{S(\theta)\leq 1}$ **and** $S(\theta) = \dfrac{(2+\cos\theta)(1-\cos\theta)^2}{4}$

Effects of terms on excess free energy: ΔG_v is negative due to lower free energy of bulk solid. Additionally solidification on the mold surface brings one more negative term - $A_{SM}\gamma_{ML}$ - due to destruction of the mould/liquid interface. Other two terms are positive as they are connected to creation of solid/liquid and solid/mould interfaces.

> iii. Sketch ($\Delta G = f(r)$) and describe the relationship between the excess free energy of solid clusters for homogeneous and heterogeneous nucleation. (2 p)
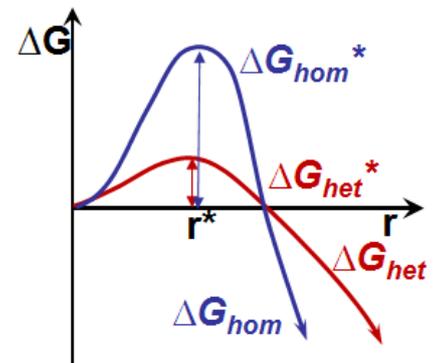> Motivation and presentation of relevant equations is necessary to get full credit (6 p)

Activation energy barrier against heterogeneous nucleation is smaller than the homogeneous one by the shape factor $\boldsymbol{S(\theta)\leq 1}$:
$$\boldsymbol{\Delta G^*_{het} = S(\theta)\Delta G^*_{hom}}$$

But the radius of the nuclei is the same:

$$r^* = \frac{2\gamma_{SL}}{\Delta G_v} \qquad \Delta G^* = \frac{16\pi\gamma_{SL}^3}{3\Delta G_v^2} S(\theta)$$

> b) Sketch and describe formation of cellular microstructure from planar solidification front during solidification. Describe temperature and solute distribution associated with cellular solidification. Motivate your answer. (4p)

Necessary condition for the formation of the stable protrusion on the planar interface is the existence of the constitutional supercooling in the liquid in front of the planar interface. At such condition break-down of the interface with formation of the cellular structure will take place. Figure indicates development of cellular structure.

CHALMERS — Chalmers University of Technology

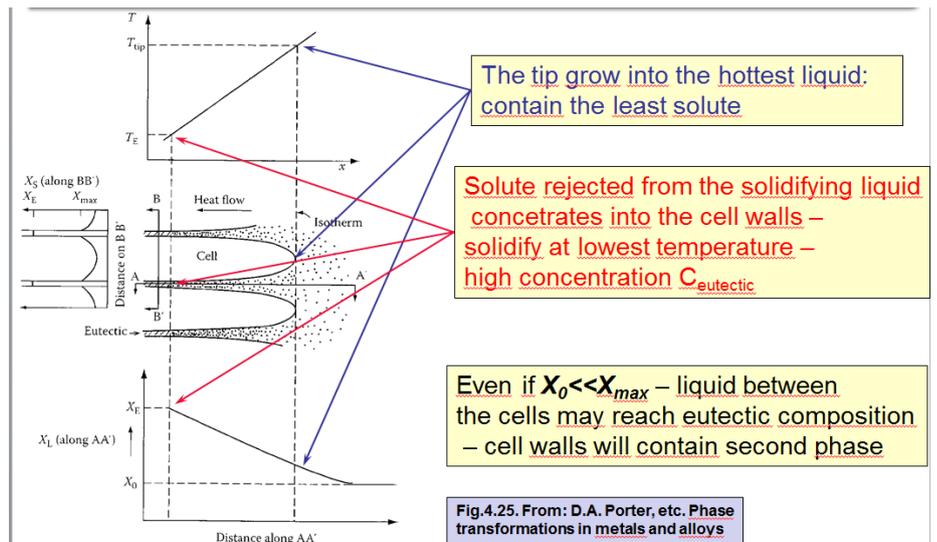## Cellular and Dendritic Solidification

Temperature gradient ahead of initial planar interface is gradually reduced below critical value → breakdown of the interface → cellular structure

$$\frac{dT_L}{dx}\bigg/v < \frac{T_1 - T_3}{D}$$

- *first protrusion – solute rejection and pile-up at the root;*
- *lower equilibrium solidification temperature – recesses formation*
- *triggering of formation of other protrusions*
- *protrusions develop into long cells – parallel to the heat flow*

- increase the amount of solute → increase of T_1-T_3 → cell structure;
- cells has virtually the same orientation as its neighbours and together they form a single grain;

Cellular microstructure is characterized by local heterogeneity in composition as the tips of the cell grow into the hottest liquid and so contain the least solute at the same time as the solute, rejected from the solidifying liquid, concentrates into the cell walls and solidifies at lowest temperatures, see Figure:
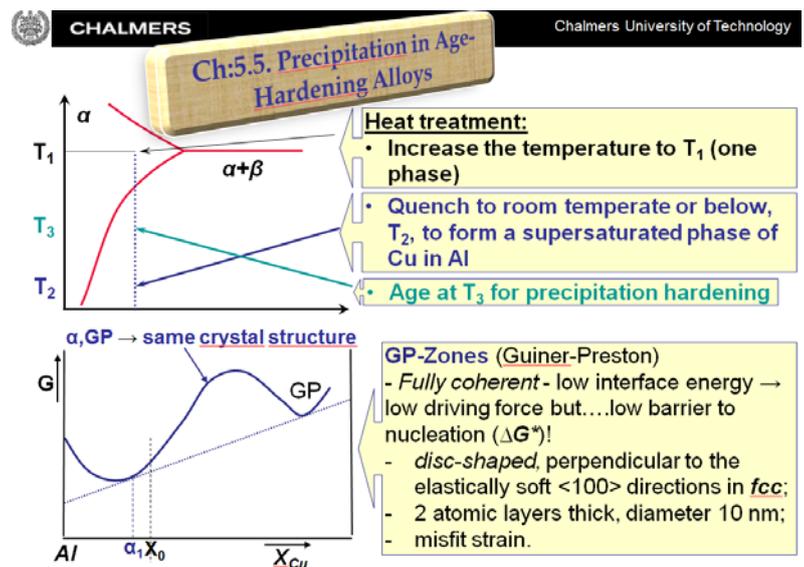

The tip grow into the hottest liquid: contain the least solute

Solute rejected from the solidifying liquid concetrates into the cell walls – solidify at lowest temperature – high concentration $C_{eutectic}$

Even if $X_0 << X_{max}$ – liquid between the cells may reach eutectic composition – cell walls will contain second phase

Fig.4.25. From: D.A. Porter, etc. Phase transformations in metals and alloys

5. Diffusional transformations (6 p).

Precipitation in age-hardening alloys:

      a. Describe thermodynamically formation of the GP zones and following precipitation of transition phases based on schematic molar free energy diagram. You can use Al-Cu system as an example (3 p)

Aging procedure, see Figure, supersaturated solid solution is aged – holded for a period of time at temperature below temperature of precipitation of metastable/stable phases and as a result fine coherent GP zones precipitate.

CHALMERS   Chalmers University of Technology

Ch:5.5. Precipitation in Age-Hardening Alloys

Heat treatment:
- Increase the temperature to T_1 (one phase)
- Quench to room temperate or below, T_2, to form a supersaturated phase of Cu in Al
- Age at T_3 for precipitation hardening

$\alpha,GP \rightarrow$ same crystal structure

GP-Zones (Guiner-Preston)
- *Fully coherent* - low interface energy $\rightarrow$ low driving force but....low barrier to nucleation (ΔG^*)!
- *disc-shaped*, perpendicular to the elastically soft <100> directions in *fcc*;
- 2 atomic layers thick, diameter 10 nm;
- misfit strain.

The precipitation of the GP zones is usually followed by precipitation of the so-called transition phases, in the sequence based on their thermodynamic stability according to Figure for Al-Cu system:

Full sequence of transformation from GP zones to equilibrium precipitate $\rightarrow$ only if alloy is aged below GP-zones solvus

9
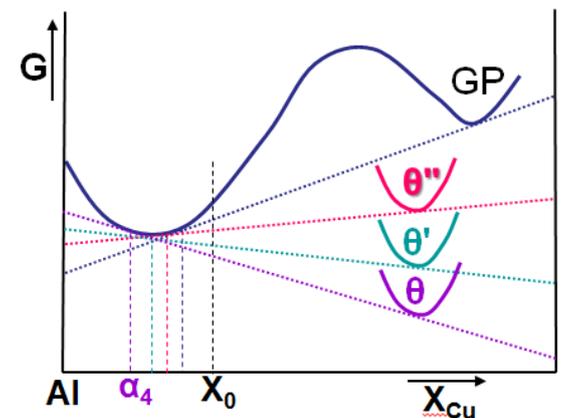
b. Describe precipitation sequence starting from GP zones to thermodynamically stable θ precipitates and describe their structure, morphology and orientational relationship to the base matrix. (3 p)

The precipitation process sequence can be presented as follows , see Figure:

GP-Zones (Guiner-Preston)
- Fully coherent - low interface energy → low driving force but….low barrier to nucleation (ΔG^*)!
- *disc-shaped,* perpendicular to the elastically soft <100> directions in *fcc*;
- 2 atomic layers thick, diameter 10 nm;
- misfit strain.

θ" *transition phase*
- fully *c*oherent but larger misfit strain;
- tetragonal unit cell – distorted *fcc* structure;
- discs 10x100 nm.

θ' *transition phase*
- broad face of plate coherent, sides not;
- tetragonal unit cell with approx. Composition $CuAl_2$;
- the same orientation relationship as *θ"*;
- 1 µm diameter;
- misfit dislocations on the broad faces;
- no long-range coherency-strain fields;
- heterogeneously nucleates on disslocations.

θ **– equilibrium phase**
- **i**ncoherent equilibrium phase;
- complex body-centered tetragonal structure;
- composition $CuAl_2$;
- high driving force but high barrier to nucleation;
- nucleates on grain boundaries or θ'/matrix interface.
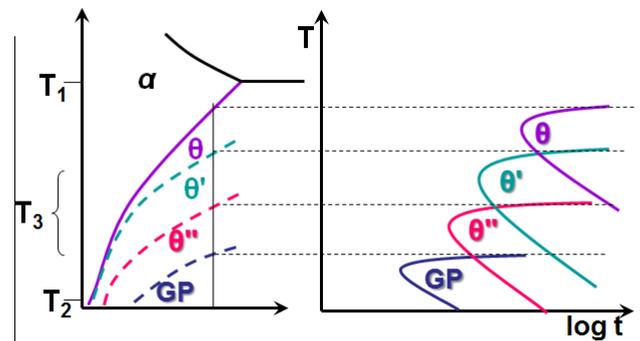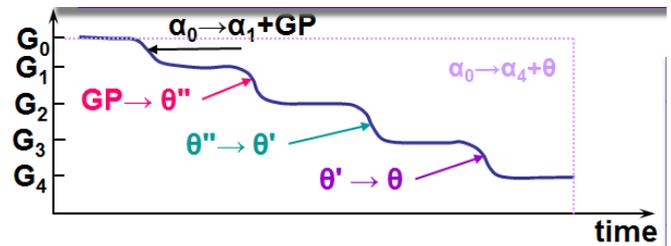
6. Diffusionless transformation (3 p)

Martensite is form from austenite at large undercooling by diffusionless transformation, or so called military transformation.
   a) Describe effect of alloying elements – namely C and Ni - on the martensite morphology, martensite start temperature and residual austenite. Describe amount of residual austenite based on martensite morphology. Motivate your answer. (3p).

- Low carbon (0.4 wt.%C) low-alloyed steels - **lath martensite** - growth by nucleation dislocations at the highly-strained interface;
- **Plate martensite** – medium and high carbon, high-nickel steels - associated with lower M_s and higher amount of retained austenite;
- medium C or Ni martensite → plates with twinned central "midrib" with outer regions being free of twins;
- high C or Ni martensite is completely twinned;

Metals Handbook -> Structure/Property Relationships in Irons and Steels -> Role of Microstructure

- carbon content significantly effects martensite transformation temperatures (both, M_s and M_f): $M_s \sim 500°C$ for low-carbon steels and considerably decreases with carbon content;
- amount of retained austenite is also considerably increases with increasing carbon content → up to 10-15% → connected to high elastic stresses between martensite plates → suppress further growth or thickening of the plates.
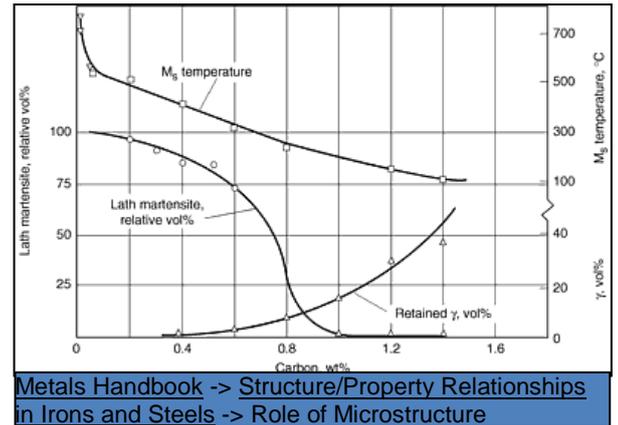
7. Novel metallic materials (3 p)

Describe basic principles of formation of metallic glasses from thermodynamic point of view and their performance advantages (3p).

1. Alloys with ≥ 3 elements → "confusion prioniciple" → atoms of significantly different sizes (>12%) → high packing density and low free volume per atom → up to orders of magnitude higher viscosity than other metals and alloys in molten state → viscosity prevents the atoms moving enough to form an ordered lattice;
2. posses high entropy and should have negative heat of mixing → stabilization of glassy state → suppress crystal nucleation and prolongs the time the molten metal stays in supercooled state → no growth;
3. "deep" eutectics with low eutectic temperature → liquid state is stable

Advantages over conventional alloys:
1. absence of grain boundaries → better resistance to wear and corrosion;
2. are also much tougher and less brittle than oxide glasses and ceramics;
3. good electrical conductivity, high yield strength, high hardness, superior strength/weight ratio, superior elastic limit, high corrosion resistance, high wear-resistance, unique acoustical properties, etc.

8. Solid/gas interactions (3 p)

During sintering of hard-metals, efficient removal of the surface cobalt oxide (CoO) from the base powder is required during initial stages of sintering. Evaluate maximum tolerable water vapour pressure in the system at T= 700°C required to provide reduction of mentioned above oxide if material is heated in Ar/H2 mix (99%Ar/1%H$_2$) and change of Gibbs free energy for this reaction is equal to $\Delta G(CoO)_{700°C}$=-28913 J [CoO+H$_2$=Co+H$_2$O]. (3p)

$$K = \frac{a_{Co}a_{H2O}}{a_{Co}a_{H2}} = \frac{p(H2O)}{p(H2)} \qquad K = \exp\left(-\frac{\Delta G°}{RT}\right) = \exp\left(-\frac{-28913}{8.314*973}\right) = 35.65$$

$p(H2O) = K * P(H2) = 35.65 * 0,01 = 0.3565\ (bar)$

Pressure of water vapor in the system do not has to exceed 0.36 bar:
$p(H2O) < 0.3565\ (bar)$